International Journal of Applied Mathematics, Sciences, and Technology for National Defense
Volume 4, Issue 1, 37-56
e_ISSN: 2985-9352, p_ISSN: 2986-0776
https://www.journal.foundae.com/index.php/JAS-ND
DOI : https://doi.org/10.58524/app.sci.def.v4i1.1136

A human–animal interaction model for monkeypox transmission dynamics: Implications for public health resilience

Vina Lusiana*
Indonesia Defense University
INDONESIA

Suhaila Saidat
Irbid National University
JORDAN

Yohana Herlina Putri
Indonesia Defense University
INDONESIA

Article Info

Article history:

Received: January 3, 2026
Revised: March 1, 2026
Accepted: April 10, 2026

Keywords:

Basic Reproduction Number
Mathematical Modeling
Monkeypox
Sensitivity Analysis
Zoonotic Transmission

Abstract

Background: Monkeypox is a zoonotic infectious disease transmitted between humans and animal reservoirs that poses a growing public health and biosecurity concern. Its transmission dynamics involve both human-to-human interactions and cross-species transmission, which may contribute to sustained outbreaks. Mathematical modeling provides a systematic framework for analyzing these dynamics and supporting strategic intervention planning.
Aims: This study aims to develop and analyze a deterministic compartmental model describing monkeypox transmission dynamics between human and rodent populations and to evaluate the impact of key epidemiological parameters on disease spread.
Methods: A system of nonlinear differential equations is formulated to represent the transmission process. The human population is classified into seven compartments (S, V, E, I, Q, H, R), while the rodent population is divided into four compartments (S, E, I, R). The basic reproduction number R_0 is derived using the next-generation matrix approach. Equilibrium analysis is conducted to determine the stability of disease-free and endemic states. Sensitivity analysis and numerical simulations are performed to assess the influence of model parameters.
Results: The analysis shows that the disease-free equilibrium is locally stable when $R_0 < 1$, indicating that the infection will die out, whereas endemic transmission persists when $R_0 > 1$. Sensitivity analysis reveals that transmission parameters, particularly β_h, β_1, and β_2, have the strongest influence on R_0. Numerical simulations demonstrate that reducing transmission rates and increasing intervention-related parameters $(\tau, \theta_2, \theta_3, v, \epsilon)$ significantly decrease the number of infected individuals and the epidemic peak. Control measures targeting rodent populations (γ_2) also contribute to reducing sustained transmission.
Conclusion: The proposed model emphasizes the critical role of integrating human health interventions with zoonotic reservoir control in mitigating monkeypox outbreaks. The findings provide a mathematical basis for supporting public health policy and strengthening national defense preparedness against emerging infectious diseases. Future research may incorporate optimal control strategies, spatial heterogeneity, and real outbreak data calibration to enhance model applicability and predictive performance.

To cite this article: Lusiana, V., Saidat, S., & Putri, Y. H. (2026). A human–animal interaction model for monkeypox transmission dynamics: Implications for public health resilience. *International Journal of Applied Mathematics, Sciences, and Technology for National Defense,* 4(1), 37-56.

***Corresponding Author:**
Vina Lusiana, Indonesia Defense University, Indonesia, Email: vina.lusiana@idu.ac.id

INTRODUCTION

Monkeypox (mpox) is a zoonotic infectious disease caused by the Monkeypox virus (MPXV), a member of the genus *Orthopoxvirus* within the family *Poxviridae*. Clinically, mpox presents with fever, lymphadenopathy, and characteristic vesiculopustular skin lesions, with varying severity depending on host immunity and viral clade (Kannan et al., 2022; Wang & Lun, 2023). Early large-scale observations across multiple countries also highlighted the global clinical spectrum and transmission patterns of the disease (Thornhill et al., 2022). In recent years, mpox has attracted increasing global attention due to its evolving epidemiology and expanding geographic distribution beyond traditionally endemic regions (Bunge et al., 2022; Chen et al., 2026). Evidence from recent outbreaks indicates that mpox is no longer confined to Central and West Africa but has been reported in multiple non-endemic regions, highlighting its broader transmission potential (Cordeiro et al., 2025; Li et al., 2025; Zhang et al., 2025). Global surveillance reports have further confirmed the continued spread of mpox across multiple regions, emphasizing its status as an emerging global health concern (WHO, 2024)

The transmission dynamics of mpox are complex, involving both human-to-human transmission and zoonotic spillover from animal reservoirs. Additionally, evidence suggests the presence of asymptomatic or subclinical infections, which may contribute to undetected transmission chains and complicate outbreak control efforts (De Baetselier et al., 2022; Rossotti et al., 2023). Small mammals, particularly rodents, are considered important in maintaining the virus in nature and facilitating cross-species transmission (Bolaji et al., 2024; Demir, 2025). In humans, infection typically begins with nonspecific prodromal symptoms followed by the appearance of characteristic skin lesions, although clinical severity may vary depending on viral and host-related factors (Nilasari et al., 2025; Tenrisau et al., 2025). Experimental and virological studies further suggest that differences in viral pathogenicity and transmissibility can influence outbreak dynamics and control efforts (Chen et al., 2026; Prévost et al., 2026; Tian et al., 2026).

Recent epidemiological developments indicate a shift in the global distribution of mpox. Increased human mobility, urbanization, and intensified human–animal interactions are among the factors associated with the spread of zoonotic diseases into new regions (Bolaji et al., 2024; El Moujaddid et al., 2025). In Southeast Asia, including Indonesia, mpox has emerged as a potential public health concern, with reported cases and indications of possible local transmission (Nilasari et al., 2025; Tenrisau et al., 2025). National reports have also documented mpox cases and response strategies in Indonesia, highlighting the need for strengthened surveillance and control measures (Kemenkes, 2024). Demographic characteristics such as high population density and mobility may further increase the risk of disease transmission (BPS-Statistics Indonesia, 2024). These conditions highlight the importance of understanding transmission dynamics, particularly the interaction between human and animal populations, to support effective control strategies.

Mathematical modelling has become an essential tool for understanding infectious disease dynamics and supporting evidence-based decision-making. Classical compartmental models, such as SIR and SEIR frameworks, provide simplified representations of disease transmission processes and enable the estimation of key epidemiological parameters (Brauer et al., 2019; Keeling & Rohani, 2019). These approaches have been widely used to evaluate intervention strategies and explore outbreak scenarios (Allehiany et al., 2023). In the context of mpox, various modelling studies have incorporated fractional-order dynamics, intervention strategies, and data-driven approaches to better capture disease complexity (Agbata et al., 2025; Onifade et al., 2025; Pesantes-Grados et al., 2025; Qian et al., 2025). Other modelling approaches have also examined the role of co-infections and population heterogeneity in shaping mpox dynamics (Omame et al., 2025), as well as the impact of border control strategies on reducing disease importation risk (Jin et al., 2025). Machine learning techniques have also been explored to enhance prediction and detection capabilities (Nivetha et al., 2025; Joshi et al., 2025; Ernest-Okonofua et al., 2025), although these approaches are generally complementary to mechanistic modeling.

Behavioral and social factors also influence mpox transmission dynamics. Studies have highlighted the role of vaccination uptake, public awareness, and behavioral responses in shaping outbreak patterns (Halder et al., 2025; Xu et al., 2025; Wu et al., 2025; Merad et al., 2025). Empirical studies have demonstrated the effectiveness of vaccines such as JYNNEOS vaccine in reducing mpox

transmission and disease severity (Azeez et al., 2022; Deputy et al., 2023). Advances in biomedical research continue to support the development of antiviral treatments and vaccines, contributing to improved prevention and control strategies (Albericio et al., 2025; Herate et al., 2025; Su et al., 2026). Many existing models primarily focus on human-to-human transmission and do not explicitly incorporate the role of animal reservoirs or bidirectional interactions between species. This limitation may reduce their ability to represent the complexity of zoonotic transmission systems.

From a national health security perspective, mathematical modelling of mpox transmission can support biosecurity threat assessment, inform preparedness planning, and contribute to the protection of populations operating in high-risk environments, including military personnel deployed in endemic or border regions. This study develops a deterministic compartmental model that integrates both human and animal populations in describing mpox transmission dynamics. The model incorporates key intervention strategies, including vaccination, quarantine, and treatment. Analytical methods include the derivation of the basic reproduction number, equilibrium stability analysis, and sensitivity analysis. The proposed framework is expected to provide insights into mpox transmission dynamics and support preparedness efforts in both public health and national defense contexts.

METHOD

Mathematical Model

This study develops a deterministic compartmental model describing the transmission dynamics of monkeypox between human and rodent populations. The proposed model is a modification of the model introduced by Bolaji et al. (2024) with the addition of a vaccination compartment. The total human population $N_h(t)$ is divided into seven epidemiological compartments $S_h(t), V_h(t), E_h(t), I_h(t), Q_h(t), H_h(t), R_h(t)$ representing susceptible, vaccinated, exposed, infectious, quarantined, hospitalized, and recovered individuals, respectively. Rodents are considered potential zoonotic reservoirs of the virus and are modeled using an SEIR framework consisting of $S_r(t), E_r(t), I_r(t), R_r(t)$ which denote susceptible, exposed, infectious, and recovered rodents. The total populations are given by $N_h = S_h + V_h + E_h + I_h + Q_h + H_h + R_h$ and $N_r = S_r + E_r + I_r + R_r$

Transmission occurs through contact with infectious humans and infected rodents. Vaccination is incorporated through two parameters: the vaccination rate $v$and the vaccine efficacy ϵ. Because vaccines are not perfectly effective, vaccinated individuals may still become infected with reduced probability $1-\epsilon$. The schematic diagram of the proposed model based on these assumptions is presented in Figure 1.

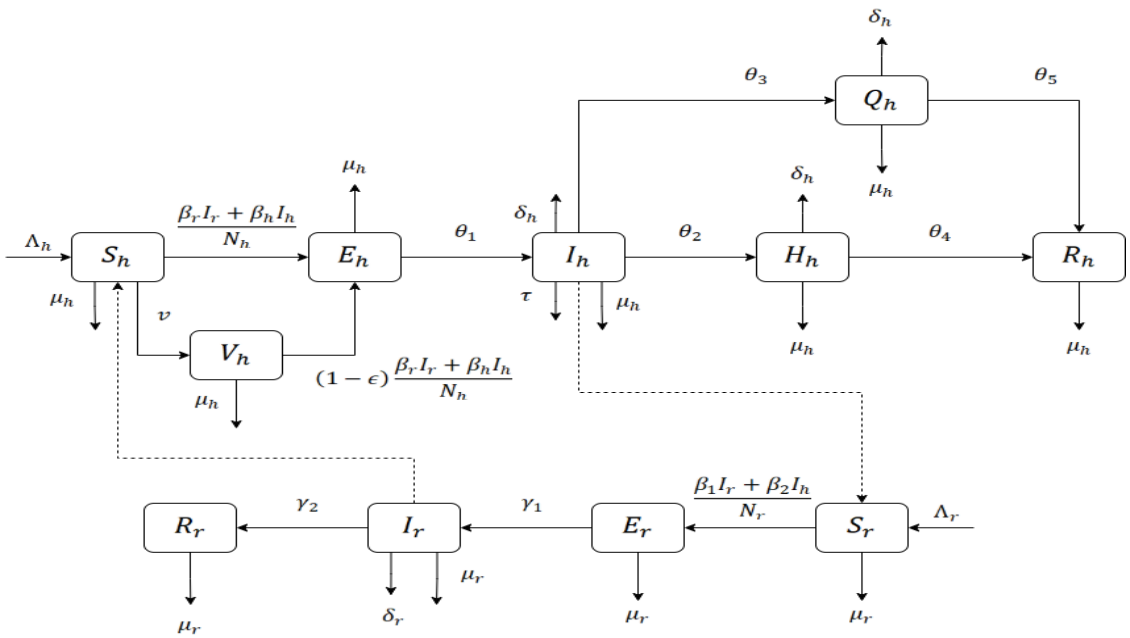

Figure 1. Schematic diagram of the SVEIQHR–SEIR monkeypox transmission model.

The differential equations system for human population is as follows:

$$\frac{dS_h}{dt} = \Lambda_h - \left(\frac{\beta_r I_r + \beta_h I_h}{N_h}\right) S_h - \upsilon S_h - \mu_h S_h \quad (1)$$

$$\frac{dV_h}{dt} = \upsilon S_h - (1-\epsilon)\left(\frac{\beta_r I_r + \beta_h I_h}{N_h}\right) V_h - \mu_h V_h \quad (2)$$

$$\frac{dE_h}{dt} = \left(\frac{\beta_r I_r + \beta_h I_h}{N_h}\right) S_h + (1-\epsilon)\left(\frac{\beta_r I_r + \beta_h I_h}{N_h}\right) V_h - (\theta_1 + \mu_h) E_h \quad (3)$$

$$\frac{dI_h}{dt} = \theta_1 E_h - (\theta_2 + \theta_3 + \mu_h + \delta_h + \tau) I_h \quad (4)$$

$$\frac{dQ_h}{dt} = (\theta_3 + \tau) I_h - (\theta_5 + \mu_h + \delta_h) Q_h \quad (5)$$

$$\frac{dH_h}{dt} = \theta_2 I_h - (\theta_4 + \delta_h + \mu_h) H_h \quad (6)$$

$$\frac{dR_h}{dt} = \theta_4 H_h + \theta_5 Q_h - \mu_h R_h \quad (7)$$

For rodents:

$$\frac{dS_r}{dt} = \Lambda_r - \left(\frac{\beta_1 I_r + \beta_2 I_h}{N_r}\right) S_r - \mu_r S_r \quad (8)$$

$$\frac{dE_r}{dt} = \left(\frac{\beta_1 I_r + \beta_2 I_h}{N_r}\right) S_r - (\mu_r + \gamma_1) E_r \quad (9)$$

$$\frac{dI_r}{dt} = \gamma_1 E_r - (\mu_r + \delta_r + \gamma_2) I_r \quad (10)$$

$$\frac{dR_r}{dt} = \gamma_2 I_r - \mu R_r \quad (11)$$

Total population:

$$N_h = S_h + V_h + E_h + I_h + Q_h + H_h + R_h \quad (12)$$

$$N_r = S_r + E_r + I_r + R_r \quad (13)$$

Based on the model system and the accompanying table, the parameter values corresponding to the SVEIQHR–SEIR model are presented in Table 1.

Table 1. Population variables and descriptions.

Variables	Description
$N_h(t)$	Total human population
$S_h(t)$	Susceptible individuals
$V_h(t)$	Vaccinated individuals
$E_h(t)$	Exposed individuals
$I_h(t)$	Infected individuals
$Q_h(t)$	Isolated individuals
$H_h(t)$	Individuals treated in hospital
$R_h(t)$	Recovered individuals
$S_r(t)$	Susceptible animals
$E_r(t)$	Exposed animals
$I_r(t)$	Infected animals

Following Table 1, the parameter values corresponding to the SVEIQHR–SEIR model structure are presented in Table 2.

Table 2. SVEIQHR-SEIR model parameter values.

Parameter	Description	Value	Source / Assumptions
Λ_h	Human population growth rate	10	(Brauer et al., 2019)
Λ_r	Rodent population recruitment rate	20	(Bolaji et al., 2024)
β_h	Human to human transmission rate	0.35 day^{-1}	(Li et al., 2025; Zhang et al., 2025)
β_r	Rodent to human transmission rate	0.15 day^{-1}	(Bolaji et al., 2024)
β_1	Rodent to rodent transmission rate	0.25 day^{-1}	(Demir, 2025)
β_2	Human to rodent transmission rate	0.2 day^{-1}	(Chen et al., 2026)
θ_1	Rate of exposure of individuals to infected individuals (incubation period ~7–14 days)	1/14 day^{-1}	(Bolaji et al., 2024; Nilasari et al., 2025)
θ_2	The rate of infected individuals admitted to hospitals (for severe cases)	1/5 day^{-1}	(Bolaji et al., 2024)
θ_3	Rate of individuals infected to quarantine (mild isolation)	1/7 day^{-1}	(Bolaji et al., 2024; Onifade et al., 2025)
θ_4	Recovery rate from hospital ($H_h \rightarrow R_h$)	1/14 day^{-1}	(Bolaji et al., 2024; Merad et al., 2025)
θ_5	Recovery rate from isolation ($Q_h \rightarrow R_h$)	1/10 day^{-1}	(Bolaji et al., 2024)
γ_1	Rate of animals exposed to infection (animal incubation ~8 days)	1/8 day^{-1}	(Chen et al., 2026)
γ_2	Rate of infected animals recovering (rodents recover in ~10 days)	1/10 day^{-1}	(Prévost et al., 2026)
τ	Human detection ($I_h \rightarrow$ isolation)	1/3 day^{-1}	(Bolaji et al., 2024; El Sharif et al., 2025)
μ_h	Natural death of humans	1/70·365 day^{-1}	(Brauer et al., 2019; BPS, 2024)
μ_r	Natural death of rodents	1/365 day^{-1}	(Demir, 2025)
δ_h	Deaths due to monkeypox in humans	0.003 day^{-1}	(Bolaji et al., 2024; Bunge et al., 2022)
δ_r	Deaths due to monkeypox in rodents	0.001 day^{-1}	(Chen et al., 2026)
ϵ	Vaccine effectiveness (if used)	0.85	(Herate et al., 2025; Su et al., 2026)
v	Vaccination rate	0.01 day^{-1}	(Wu et al., 2025)

RESULTS AND DISCUSSION

Feasible Region

Theorem 1 (Feasible Region). Suppose the solution of the SVEIQHR-SEIR human and rodent population dynamics model with non-negative initial conditions. Then, the model solution will remain bounded and non-negative for all time $t \geq 0$, and will lie within the following region:

$$\phi = \omega_h \times \omega_r \subset \Re^{+11} \tag{14}$$

with,

$$\omega_h = \left\{(S_h, V_h, E_h, I_h, Q_h, H_h, R_h) \in \mathbb{R}_+^7 \middle| N_h(t) \leq \frac{\Lambda_h}{\mu_h}\right\} \tag{15}$$

$$\omega_r = \left\{(S_r, E_r, I_r, R_r) \in \mathbb{R}_+^4 \middle| N_r(t) \leq \frac{\Lambda_r}{\mu_r}\right\} \quad (16)$$

where,

$$N_h(t) = S_h + V_h + E_h + I_h + Q_h + H_h + R_h \quad (17)$$
$$N_r(t) = S_r + E_r + I_r + R_r \quad (18)$$

Proof. For human population,

$$\frac{dN_h}{dt} = \Lambda_h - \mu_h N_h - \delta_h(I_h + Q_h + H_h) \leq \Lambda_h - \mu_h N_h \Rightarrow N_h(t) \leq \frac{\Lambda_h}{\mu_h}, \forall t \geq 0 \quad (19)$$

For rodent population,

$$\frac{dN_r}{dt} = \Lambda_r - \mu_r N_r - \delta_r I_r \leq \Lambda_r - \mu_r N_r \Rightarrow N_r(t) \leq \frac{\Lambda_r}{\mu_r}, \forall t \geq 0 \quad (20)$$

and because all compartments originate from non-negative initial conditions, and the model does not contain purely negative terms for all $t \geq 0$, $x(t) \in \mathbb{R}_+^{11}$, and $x(t) \in \phi$, $\forall t \geq 0$, the ϕ region is a closed non-negative invariant region of the system, which guarantees that the solution of this epidemiological model remains biologically meaningful (the population is non-negative and does not explode to infinity) for all times.

Disease Free Equilibrium

Disease free equilibrium (DFE) is the equilibrium point when there is no infection in the population, namely:

$$E_h = I_h = Q_h = H_h = E_r = I_r = 0 \quad (21)$$

This means that only the susceptible (S), vaccinated (V), and recovered (R) compartments have positive values. DFE ε_0 point of the system:

$$\varepsilon_0 = \left(S_h^0, V_h^0, E_h^0 = 0, I_h^0 = 0, Q_h^0 = 0, H_h^0 = 0, R_h^0, S_r^0, E_r^0 = 0, I_r^0 = 0, R_r^0\right) \quad (22)$$

where,

$$\frac{dS_h}{dt} = \Lambda_h - vS_h - \mu_h S_h = 0 \Rightarrow S_h^0 = \frac{\Lambda_h}{v + \mu_h} \quad (23)$$
$$\frac{dV_h}{dt} = vS_h - \mu_h V_h = 0 \Rightarrow V_h^0 = \frac{v}{\mu_h} S_h^0 = \frac{v\Lambda_h}{\mu_h(v + \mu_h)} \quad (24)$$
$$\frac{dR_h}{dt} = 0 - \mu_h R_h = 0 \Rightarrow R_h^0 = 0 \quad (25)$$
$$\frac{dS_r}{dt} = \Lambda_r - \mu_r S_r = 0 \Rightarrow S_r^0 = \frac{\Lambda_r}{\mu_r} \quad (26)$$
$$\frac{dR_r}{dt} = \mu_r R_r = 0 \Rightarrow R_r^0 = 0 \quad (27)$$

So that the point DFE:

$$\varepsilon_0 = \left(S_h^0, V_h^0, 0,0,0,0,0, S_r^0, 0,0,0\right) = \left(\frac{\Lambda_h}{v + \mu_h}, \frac{v\Lambda_h}{\mu_h(v + \mu_h)}, 0,0,0,0,0, \frac{\Lambda_r}{\mu_r}, 0,0,0\right) \quad (28)$$

Endemic Equilibrium

The endemic equilibrium represents a steady state where the disease persists in the population with non-zero infected compartments. Let $\Phi^* = (S_h^*, V_h^*, E_h^*, I_h^*, Q_h^*, H_h^*, R_h^*, S_r^*, E_r^*, I_r^*, R_r^*)$ denote the endemic equilibrium of the system, where all state variables are positive. The endemic equilibrium is obtained by solving the nonlinear algebraic system obtained by setting $\frac{dX}{dt} = 0$ for all compartments X. Thus, the system:

$$S_h^* = \frac{\Lambda_h(\theta_2 + \theta_3 + \mu_h + \delta_h + \tau)}{v\tau + v\delta_h + v\mu_h + v\theta_2 + v\theta_3 + \tau\mu_h + \delta_h\mu_h + \mu_h^2 + \mu_h\theta_2 + \mu_h\theta_3} \tag{29}$$

$$V_h^* = \frac{v\Lambda_h(\tau + \delta_h + \mu_h + \theta_2 + \theta_3)^2}{\epsilon v(\tau + \delta_h + \mu_h + \theta_2 + \theta_3) + \epsilon\mu_h\big(\beta_h\theta_1 + \beta_r(\tau + \delta_h + \mu_h + \theta_2 + \theta_3)\big)^2} \tag{30}$$

$$E_h^* = \frac{\beta_h + \mu_h}{(\beta_r + \beta_h) + (\theta_2 + \theta_3 + \mu_h + \delta_h)}(S_h^* + V_h^*) \tag{31}$$

$$I_h^* = \frac{\theta_1 E}{\theta_2 + \theta_3 + \mu_h + \delta_h + \tau} \tag{32}$$

$$Q_h^* = \frac{\theta_3\theta_1}{(\tau + \theta_3 + \theta_2)\delta_h + \theta_5(\tau + \delta_h + \mu_h + \delta_h^2 + \theta_2 + \theta_3) + (\delta_h + \theta_3 + \theta_2 + \mu_h + \tau)\mu_h} \tag{33}$$

$$H_h^* = \frac{\theta_2\theta_1}{(\tau + 2\mu_h + \delta_h + \theta_2 + \theta_3 + \theta_4)\delta_h + (\tau + \mu_h + \theta_2 + \theta_3 + \theta_4)\mu_h + (\tau + \theta_2 + \theta_3)\theta_4} \tag{34}$$

$$R_h^* = \mu_h\delta_h\frac{\theta_1 E}{\theta_2 + \theta_3 + \mu_h + \delta_h + \tau} + \gamma_1\frac{\theta_3\theta_1}{(\tau + \theta_3 + \theta_2)\delta_h + \theta_5(\tau + \delta_h + \mu_h + \delta_h^2 + \theta_2 + \theta_3)} + \gamma_2\frac{\theta_2\theta_1}{(\tau + 2\mu_h + \delta_h + \theta_2 + \theta_3 + \theta_4)\delta_h} \tag{35}$$

$$S_r^* = \frac{(\delta_r + \gamma_1 + \gamma_2 + \mu_r)\Lambda_r}{\gamma_1(\beta_h + \beta_r - \delta_r - \gamma_2)} \tag{36}$$

$$E_r^* = \frac{(\beta_h\gamma_1 + \beta_r\gamma_1 - \delta_r\gamma_1 - \delta_r\mu_r - \gamma_1\gamma_2 - \gamma_1\mu_r - \gamma_2\mu_r - \mu_r^2)\Lambda_r}{\gamma_1(\beta_h\gamma_1 + \beta_h\mu_r + \beta_r\gamma_1 + \beta_r\mu_r - \delta_r\gamma_1 - \delta_r\mu_r - \gamma_1\gamma_2 - \gamma_2\mu_r)} \tag{37}$$

$$I_r^* = \frac{(\beta_h\gamma_1 + \beta_r\gamma_1 - \delta_r\gamma_1 - \gamma_2\mu_r - \mu_r^2)\Lambda_r}{\beta_h\beta_r\delta_r\gamma_1\gamma_2(\delta_r\gamma_1 + \beta_h\delta_r\mu_r + \beta_h\gamma_1\gamma_2 + \beta_h\gamma_1\mu_r + \beta_h\gamma_2\mu_r + \beta_r\mu_r^2)} \tag{38}$$

$$R_r^* = \frac{\gamma_2(\beta_h\gamma_1 + \beta_r\gamma_1 - \delta_r\gamma_1 - \gamma_2\mu_r - \mu_r^2)\Lambda_r}{(\delta_r\gamma_1 + \beta_h\delta_r\mu_r + \beta_h\gamma_1\gamma_2 + \beta_h\gamma_1\mu_r + \beta_h\gamma_2\mu_r + \beta_r\mu_r^2)\mu_r} \tag{39}$$

Basic Reproduction Number Point (R_0)

The basic reproduction number, symbolized by R_0, is an important parameter that it indicates the average number of secondary infections transmitted by one infected individual to a completely susceptible population. This value determines whether a disease can spread in a population or not. The R_0 value is calculated using the next-generation operator approach under the free infection equilibrium (DFE) condition, through the next-generation matrix method. In this method, two matrices are formed: one to describe the rate of new infections, and another for transitions between other compartments. We focus only on the compartments that play a role in the spread of infection, namely: For humans: E_h, I_h and rodents: E_r, I_r.

So, the infectious status vector is:

$$x = \begin{bmatrix} E_h \\ I_h \\ E_r \\ I_r \end{bmatrix} \tag{40}$$

Next, the form of the new infection rate vector $\mathcal{F}$ and the transition rate $\mathcal{V}$:

$$\mathcal{F} = \begin{bmatrix} \left(\frac{\beta_r I_r + \beta_h I_h}{N_h}\right) S_h + (1-\epsilon)\left(\frac{\beta_r I_r + \beta_h I_h}{N_h}\right) V_h \\ 0 \\ \left(\frac{\beta_1 I_r + \beta_2 I_h}{N_r}\right) S_r \\ 0 \end{bmatrix} \tag{41}$$

$$\mathcal{V} = \begin{bmatrix} (\theta_1 + \mu_h) E_h \\ -\theta_1 E_h + (\theta_2 + \theta_3 + \mu_h + \delta_h + \tau) I_h \\ (\gamma_1 + \mu_r) E_r \\ -\gamma_1 E_r + (\mu_r + \delta_r + \gamma_2) I_r \end{bmatrix} \tag{42}$$

In DFE: $(E_h = I_h = Q_h = H_h = R_h = 0)$ and $(E_r = I_r = R_r = 0)$, all populations are only in the susceptible and vaccinated compartments, $N_h = S_h^0 + V_h^0$ and $N_r = S_r^0$.

Define $x = [E_h \quad I_h \quad E_r \quad I_r]^T$

$$F = \begin{bmatrix} 0 & \frac{\beta_h S_h^0 + (1-\epsilon)\beta_h V_h^0}{N_h} & 0 & \frac{\beta_r S_h^0 + (1-\epsilon)\beta_r V_h^0}{N_h} \\ 0 & 0 & 0 & 0 \\ 0 & \frac{\beta_2 S_r^0}{N_r} & 0 & \frac{\beta_1 S_r^0}{N_r} \\ 0 & 0 & 0 & 0 \end{bmatrix} \tag{43}$$

$$V = \begin{bmatrix} \theta_1 + \mu_h & 0 & 0 & 0 \\ -\theta_1 & \theta_2 + \theta_3 + \mu_h + \delta_h + \tau & 0 & 0 \\ 0 & 0 & \gamma_1 + \mu_r & 0 \\ 0 & 0 & -\gamma_1 & \mu_r + \delta_r + \gamma_2 \end{bmatrix} \tag{44}$$

Since F and V are 4×4, we can take the non-zero part of F and V to calculate the largest eigenvalue of $K = FV^{-1}$, which is the value of R_0. However, because it is block diagonal, we can separate it into two sub-populations:

Human population (R_0^h),

$$\mathrm{R}_0^{(h)} = \frac{\beta_h \theta_1 (\mu_h + \upsilon(1-\epsilon))}{(\mu_h + \upsilon)(\theta_1 + \mu_h)(\theta_2 + \theta_3 + \mu_h + \delta_h + \tau)} \tag{45}$$

Rodent population (R_0^r),

$$\mathrm{R}_0^{(r)} = \frac{\beta_1 \gamma_1}{(\mu_r + \gamma_1)(\mu_r + \delta_r + \gamma_2)} \tag{46}$$

If cross-infection between humans and rodents is considered, the total basic reproduction number cannot be expressed as a simple sum of $R_0^{(h)}$ and $R_0^{(r)}$. Instead, it is defined as the spectral radius of the next-generation matrix:

$$R_0 = \rho(FV^{-1})$$

$$R_0 = \frac{1}{2}\left[\mathrm{R}_0^{(h)} + \mathrm{R}_0^{(r)} + \sqrt{\left(\mathrm{R}_0^{(h)} - \mathrm{R}_0^{(r)}\right)^2 + 4R_{hr}R_{rh}}\right] \tag{47}$$

with cross-infection terms:

$$R_{hr} = \frac{\beta_r \theta_1 (\mu_h + \upsilon(1-\epsilon))}{(\mu_h + \upsilon)(\theta_1 + \mu_h)(\theta_2 + \theta_3 + \mu_h + \delta_h + \tau)} \tag{48}$$

$$R_{rh} = \frac{\beta_2 \gamma_1}{(\mu_r + \gamma_1)(\mu_r + \delta_r + \gamma_2)}$$

The explicit form of the basic reproduction number shows that the overall disease dynamics are governed not only by within-population transmission but also by cross-species interactions, which may significantly amplify the epidemic potential.

Local Stability of the Disease-Free Equilibrium

Theorem 2. The disease-free equilibrium $\varepsilon_0$is locally asymptotically stable if $R_0 < 1$and unstable if $R_0 > 1$.

Proof. The Jacobian matrix of the infected subsystem evaluated at the disease-free equilibrium yields the next-generation matrix $K = FV^{-1}$. The stability of the disease-free equilibrium depends on the spectral radius of K. If $R_0 < 1$, all eigenvalues of the Jacobian matrix have negative real parts, implying that the disease-free equilibrium is locally asymptotically stable. Conversely, if $R_0 > 1$, the infection can invade the population and the disease-free equilibrium becomes unstable.

Local Stability of the Endemic Equilibrium

To analyze local stability around the endemic equilibrium point, a Jacobian matrix J is formed from the system mentioned above, then evaluated at the endemic equilibrium point. Next, it is assumed that:

$$f_1 = \frac{dS_h}{dt} = \Lambda_h - \left(\frac{\beta_r I_r + \beta_h I_h}{N_h}\right) S_h - vS_h - \mu_h S_h \quad (49)$$

$$f_2 = \frac{dV_h}{dt} = vS_h - (1-\epsilon)\left(\frac{\beta_r I_r + \beta_h I_h}{N_h}\right) V_h - \mu_h V_h \quad (50)$$

$$f_3 = \frac{dE_h}{dt} = \left(\frac{\beta_r I_r + \beta_h I_h}{N_h}\right) S_h + (1-\epsilon)\left(\frac{\beta_r I_r + \beta_h I_h}{N_h}\right) V_h - (\theta_1 + \mu_h) E_h \quad (51)$$

$$f_4 = \frac{dI_h}{dt} = \theta_1 E_h - (\theta_2 + \theta_3 + \mu_h + \delta_h + \tau) I_h \quad (52)$$

$$f_5 = \frac{dQ_h}{dt} = \theta_3 I_h - (\theta_5 + \mu_h + \delta_h) Q_h \quad (53)$$

$$f_6 = \frac{dH_h}{dt} = \theta_2 I_h - (\theta_4 + \delta_h + \mu_h) H_h \quad (54)$$

$$f_7 = \frac{dR_h}{dt} = \theta_4 H_h + \theta_5 Q_h - \mu_h R_h \quad (55)$$

$$f_8 = \frac{dS_r}{dt} = \Lambda_r - \left(\frac{\beta_1 I_r + \beta_2 I_h}{N_r}\right) S_r - \mu_r S_r \quad (56)$$

$$f_9 = \frac{dE_r}{dt} = \left(\frac{\beta_1 I_r + \beta_2 I_h}{N_r}\right) S_r - (\mu_r + \gamma_1) E_r \quad (57)$$

$$f_{10} = \frac{dI_r}{dt} = \gamma_1 E_r - (\mu_r + \delta_r + \gamma_2) E_r \quad (58)$$

$$f_{11} = \frac{dR_r}{dt} = \gamma_2 I_r + \mu R_r \quad (59)$$

with total population,

$$N_h = S_h + V_h + E_h + I_h + Q_h + H_h + R_h \quad (60)$$

$$N_r = S_r + E_r + I_r + R_r \quad (61)$$

Jacobian matrix:

$$J = \begin{bmatrix} \alpha_{11} & \alpha_{12} & \alpha_{13} & \alpha_{14} & \alpha_{15} & \cdots & \alpha_{1,11} \\ \alpha_{21} & \alpha_{22} & \alpha_{23} & \alpha_{24} & \alpha_{25} & \cdots & \alpha_{2,11} \\ \alpha_{31} & \alpha_{32} & \alpha_{33} & \alpha_{34} & \alpha_{35} & \cdots & \alpha_{3,11} \\ \alpha_{41} & \alpha_{42} & \alpha_{43} & \alpha_{44} & \alpha_{45} & \cdots & \alpha_{4,11} \\ \alpha_{51} & \alpha_{52} & \alpha_{53} & \alpha_{54} & \alpha_{55} & \cdots & \alpha_{5,11} \\ \vdots & \vdots & \vdots & \vdots & \vdots & \ddots & \vdots \\ \alpha_{11,1} & \alpha_{11,2} & \alpha_{11,3} & \alpha_{11,4} & \alpha_{11,5} & \cdots & \alpha_{11,11} \end{bmatrix} \quad (62)$$

with,

$\alpha_{11} = -\frac{\beta_h I_h + \beta_r I_r}{N_h} - v - \mu_h;\ \alpha_{14} = -\frac{\beta_h S_h}{N_h};\ \alpha_{1,10} = -\frac{\beta_r S_h}{N_h};$
$\alpha_{21} = v;\ \alpha_{22} = -\frac{(1-\epsilon)(\beta_h I_h + \beta_r I_r)}{N_h} - \mu_h;\ \alpha_{24} = -\frac{(1-\epsilon)\beta_h V_h}{N_h};\ \alpha_{2,10} = -\frac{(1-\epsilon)\beta_r V_h}{N_h};$
$\alpha_{31} = \frac{\beta_h I_h + \beta_r I_r}{N_h};\ \alpha_{32} = \frac{(1-\epsilon)(\beta_h I_h + \beta_r I_r)}{N_h};\ \alpha_{33} = -\theta_1 - \mu_h;\ \alpha_{34} = \frac{\beta_h S_h + (1-\epsilon)\beta_h V_h}{N_h};$
$\alpha_{3,10} = \frac{\beta_r S_h + (1-\epsilon)\beta_r V_h}{N_h};\ \alpha_{43} = \theta_1;\ \alpha_{44} = -\theta_2 - \theta_3 - \mu_h - \delta_h - \tau;\ \alpha_{54} = \theta_3;\ \alpha_{55} = -\theta_5 - \mu_h - \delta_h;$
$\alpha_{64} = \theta_2;\ \alpha_{66} = -\theta_4 - \delta_h - \mu_h;\ \alpha_{75} = \theta_5;\ \alpha_{76} = \theta_4;\ \alpha_{77} = -\mu_h;$
$\alpha_{84} = -\frac{\beta_2 S_r}{N_r};\ \alpha_{88} = -\frac{\beta_1 I_r + \beta_2 I_h}{N_r} - \mu_r;\ \alpha_{8,10} = -\frac{\beta_1 S_r}{N_r};$
$\alpha_{94} = \frac{\beta_2 S_r}{N_r};\ \alpha_{98} = \frac{\beta_1 I_r + \beta_2 I_h}{N_r};\ \alpha_{99} = -\mu_r - \gamma_1;\ \alpha_{9,10} = \frac{\beta_1 S_r}{N_r};$
$\alpha_{10,9} = \gamma_1;\ \alpha_{10,10} = -\mu_r - \delta_r - \gamma_2;\ \alpha_{11,10} = \gamma_2;\ \alpha_{11,11} = -\mu_r,$
for other values of α_{ij} equal to 0.

Local stability will be determined using the linearization method (Keeling & Rohani, 2019). Therefore, the Jacobian matrix J_{ε_0} of the model system (1) is given as follows:

$$J_{\mathcal{E}_0} = \begin{bmatrix} -\nu - \mu_h & 0 & 0 & -d_1 & 0 & 0 & 0 & 0 & 0 & -d_2 & 0 \\ \nu & -\mu_h & 0 & -d_3 & 0 & 0 & 0 & 0 & 0 & -d_4 & 0 \\ 0 & 0 & -\theta_1 - \mu_h & d_5 & 0 & 0 & 0 & 0 & 0 & d_6 & 0 \\ 0 & 0 & 0 & -\theta_2 - \theta_3 - \mu_h - \delta_h - \tau & 0 & 0 & 0 & 0 & 0 & 0 & 0 \\ 0 & 0 & 0 & \theta_3 & -\theta_5 - \mu_h - \delta_h & 0 & 0 & 0 & 0 & 0 & 0 \\ 0 & 0 & 0 & \theta_2 & 0 & -\theta_4 - \mu_h - \delta_h & 0 & 0 & 0 & 0 & 0 \\ 0 & 0 & 0 & 0 & \theta_5 & \theta_4 & -\mu_h & 0 & 0 & 0 & 0 \\ 0 & 0 & 0 & 0 & 0 & 0 & 0 & -\mu_r & 0 & -d_7 & 0 \\ 0 & 0 & 0 & 0 & 0 & 0 & 0 & 0 & -\mu_r - \gamma_1 & d_8 & 0 \\ 0 & 0 & 0 & 0 & 0 & 0 & 0 & 0 & \gamma_1 & -\mu_r - \delta_r - \gamma_2 & 0 \\ 0 & 0 & 0 & 0 & 0 & 0 & 0 & 0 & 0 & \gamma_2 & -\mu_r \end{bmatrix}$$

where

$$d_1 = \frac{\beta_h \Lambda_h}{\mu_h + v};\ d_2 = \frac{\beta_r \Lambda_h}{\mu_h + v};\ d_3 = \frac{(1-\epsilon)\beta_h v \Lambda_h}{\mu_h(\mu_h + v)};\ d_3 = \frac{(1-\epsilon)\beta_r v \Lambda_h}{\mu_h(\mu_h + v)};$$
$$d_5 = \frac{\beta_h \Lambda_h}{\mu_h + v} + \frac{(1-\epsilon)\beta_h v \Lambda_h}{\mu_h(\mu_h + v)};\ d_6 = \frac{\beta_r \Lambda_h}{\mu_h + v} + \frac{(1-\epsilon)\beta_r v \Lambda_h}{\mu_h(\mu_h + v)};\ d_7 = d_8 = \frac{(\beta_h + \beta_r)\Lambda_h}{\mu_r}$$

The eigenvalues are,

$$\lambda_1 = -v - \mu_h;\ \lambda_2 = -\mu_h;\ \lambda_3 = -\theta_1 - \mu_h;\ \lambda_4 = -\theta_2 - \theta_3 - \mu_h - \delta_h - \tau;\ \lambda_5 = -\theta_5 - \mu_h - \delta_h;$$
$$\lambda_6 = -\theta_4 - \delta_h - \mu_h;\ \lambda_7 = -\mu_h;\ \lambda_8 = -\mu_r;\ \lambda_9 = -\mu_r - \gamma_1;\ \lambda_{10} = -\mu_r - \delta_r - \gamma_2;\ \lambda_{11} = -\mu_r$$

From the calculation of the eigenvalue, it is obtained that all real parts are negative. This means that the equilibrium point of monkeypox transmission is asymptotically stable.

Experimental Results

Sensitivity analysis assesses how changes in a model parameter affect a specific output, in this case, the basic reproduction number R_0, while other parameters are held constant (Onifade et al., 2025; Omame et al., 2025). The normalized forward sensitivity index is the ratio of the relative change in R_0 to the relative change in a model parameter. If R_0 is differentiable with respect to that parameter, then the sensitivity index can be derived using partial derivatives. The parameter values used in this analysis are based on literature and are shown in Table 1. Since R_0 provides an initial picture of the potential spread of the disease, a sensitivity analysis was performed to identify which parameters have the most significant relative influence on R_0. For this purpose, the elasticity form.

$$\Upsilon_v^{R_0} = \frac{\partial R_0}{\partial p} \cdot \frac{p}{R_0} \tag{63}$$

was used, where p denotes the parameter being tested, including the vaccination parameter v and vaccine effectiveness ϵ, which directly affect the human component of R_0.

Table 3 shows the results of numerical sensitivity analysis of the basic reproduction number R_0 to model parameters.

Table 3. Sensitivity index to parameters.

Parameters	Sensitivity Value	Parameters	Sensitivity Value
β_1	0.5412	μ_r	-0.0466
β_2	0.4329	δ_h	-0.00011
γ_2	-0.9391	θ_1	0.0000101
γ_1	0.0209	θ_4	0
β_h	0.0181	θ_5	0
β_r	0.0078	μ_h	0.000546
τ	-0.0127	v	-0.000557
θ_2	-0.0076	ϵ	-0.14298
θ_3	-0.0054	$r = \frac{v + \mu_h}{v}$	0.14298
δ_r	-0.0094		

From Table 3, we can form bar chart as shown in Figure 2.

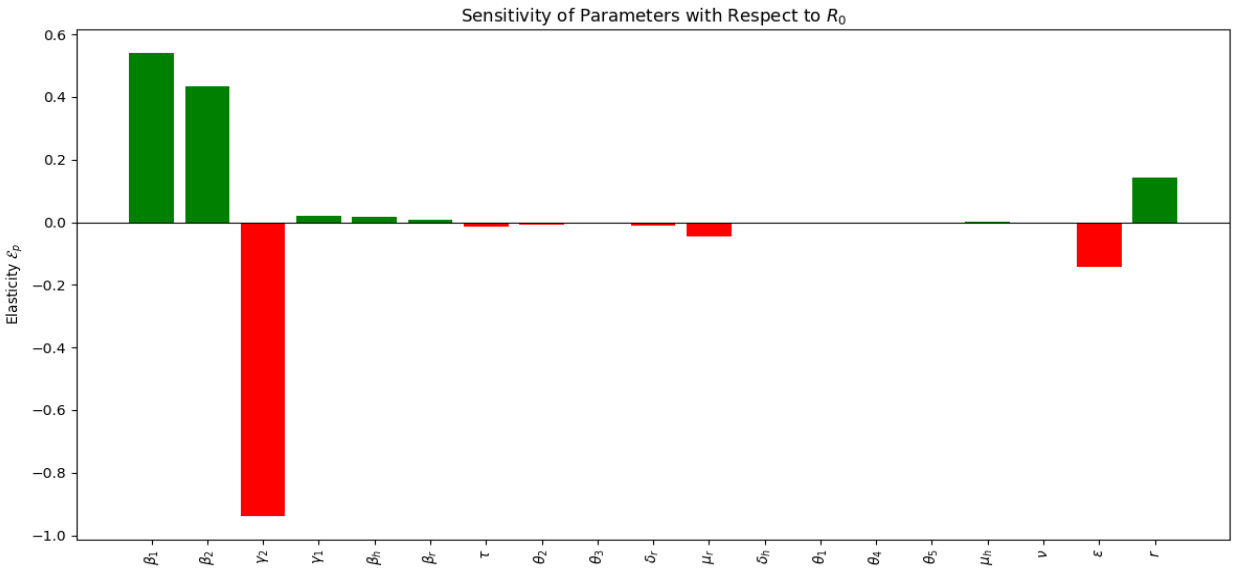

Figure 2. Sensitivity parameter to R_0.

The sensitivity index values are shown in Table 2. Based on Table 2 and Figure 1, parameters with negative sensitivity indices, such as the diagnosis rate τ, the treatment or isolation rate θ_2 and θ_3, human mortality due to infection δ_h, and the rodent recovery parameter γ_2, indicate that increasing these parameters reduces the R_0 value. Conversely, parameters with positive sensitivity indices, such as the human-to-human transmission rate β_h, the rodent-to-human transmission rate β_r, and the inter-rodent transmission rates β_1 and β_2, indicate that increasing these parameter values could increase monkeypox cases by raising the R_0 value. To evaluate the effect of the basic reproduction number R_0 on the hospital admission rate parameter θ_2 and the quarantine rate parameter θ_3, we construct a three-dimensional surface of R_0. If an explicit analytical derivative of R_0 is available, the surface can be built directly from that formula. If no analytical expression exists, the value of R_0 is calculated numerically by holding all other parameters at fixed values according to the parameter table, then varying only θ_2 and θ_3 within biologically relevant ranges.

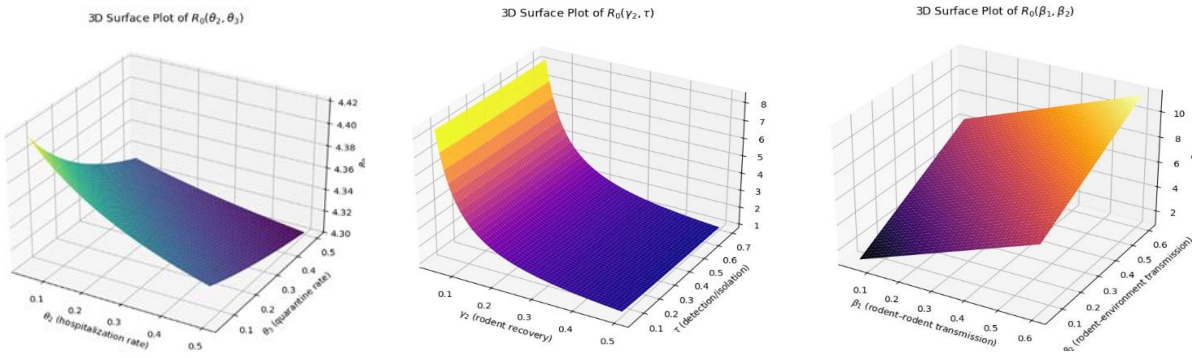

(a) (b) (c)

Figure 3. (a) 3D simulation of the effect of R_0 on the parameters θ_2 and θ_3, (b) 3D simulation of the effect of R_0 on the parameters γ_2 and τ, and (c) 3D simulation of the effect of R_0 on the parameters β_1 and β_2.

The three-dimensional simulation results presented in Figure 3 illustrate how several key parameters influence the basic reproduction number R_0. As shown in Figure 3(a), increasing the hospitalization rate for severe cases (θ_2) and the quarantine rate for mild cases (θ_3) leads to a reduction in R_0. However, the decrease is nonlinear, with a stronger impact observed at lower parameter values, while the effect gradually diminishes as the parameters increase. A similar trend is observed in Figure 3(b), where increases in the rodent recovery rate (γ_2) and the diagnosis or isolation rate in humans (τ) also contribute to reducing the value of R_0. Among these parameters, $\gamma_2$exhibits a stronger influence, indicating that reducing the infectious period within the rodent population can significantly suppress disease transmission. In contrast, Figure 3(c) shows that increasing the rodent transmission parameters β_1 and β_2 leads to a substantial increase in R_0. This result highlights the important role of rodent-to-rodent transmission and environmental transmission in sustaining the spread of monkeypox.

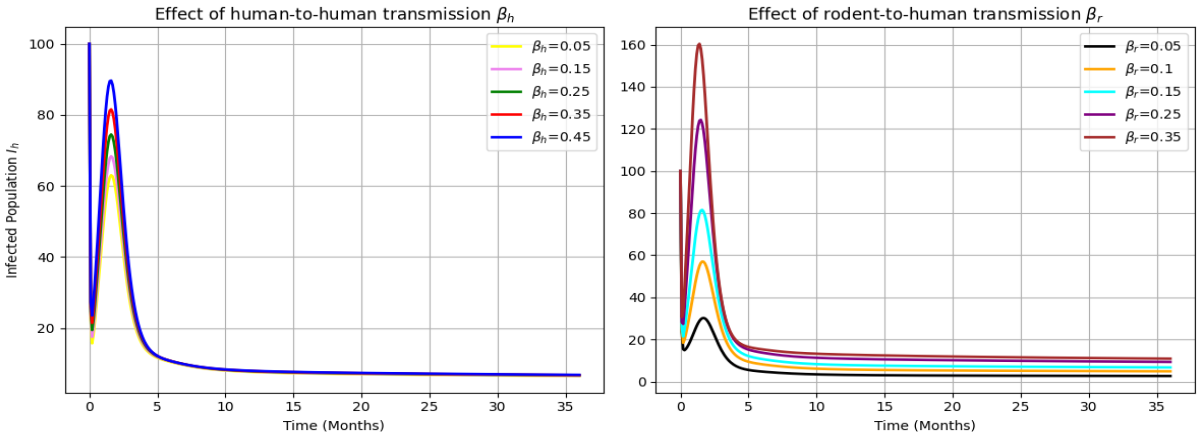

Figure 4. Population dynamics infected in the β_h and β_r scenarios.

Figure 4 illustrates the dynamics of the infected human population $I_h(t)$over a period of 36 months under different combinations of the human-to-human transmission rate (β_h) and the rodent-to-human transmission rate (β_r). In general, higher values of $\beta_h$and $\beta_r$lead to a faster increase in the infection curve, resulting in a higher peak and a larger total number of cases during the simulation period. Conversely, lower values of these parameters produce flatter curves with lower peaks and slower transmission dynamics. These results indicate that both transmission parameters play a critical role in determining the speed and magnitude of monkeypox spread in the human population. Even small increases in $\beta_h$and $\beta_r$can significantly amplify the number of cases and the intensity of outbreaks. To further examine the dynamics of disease transmission, numerical simulations were conducted by varying several key parameters while keeping the others fixed. The parameters considered include the vaccination rate v, vaccine effectiveness ϵ, the treatment or isolation transition rate τ, the disease-induced mortality rate δ_h, and the transmission parameters $\beta_h$and β_r.

In each simulation scenario, only one parameter was varied while all other parameters remained constant. This approach allows the independent influence of each parameter on the infection dynamics to be clearly observed. The simulation results provide a quantitative description of how different epidemiological mechanisms contribute to the evolution of monkeypox outbreaks and help identify parameters that are most effective in reducing infection levels.

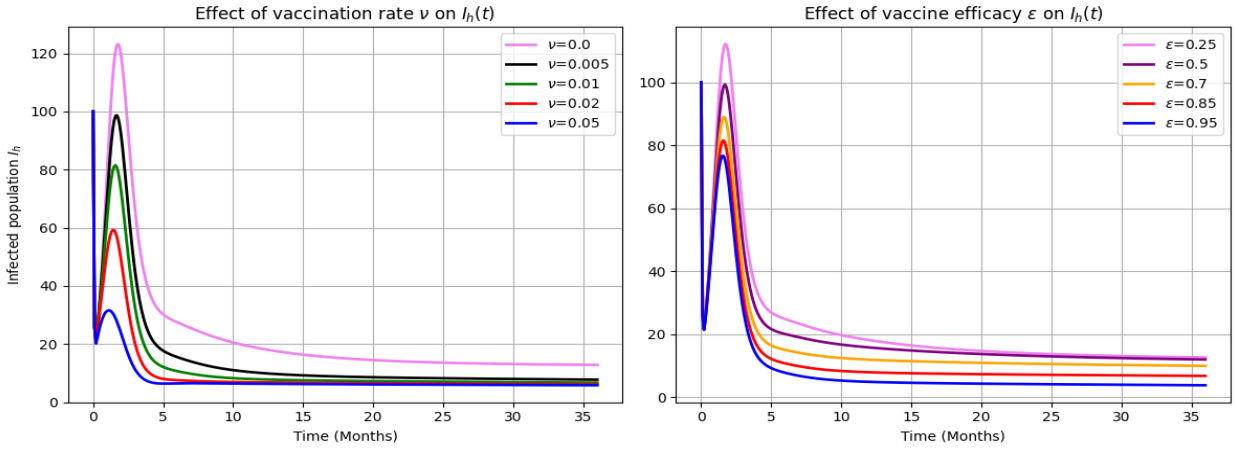

Figure 5. Population dynamics infected in the v and ϵ scenarios.

As shown in Figure 5, variations in the vaccination rate v and vaccine effectiveness ϵ significantly influence the dynamics of infected individuals $I_h(t)$. Higher values of both parameters consistently reduce the magnitude of the outbreak. Under scenarios with larger $v$or ϵ, the infection curve remains at a lower level throughout the simulation, with a smaller peak and a slower growth of cases. This pattern indicates that increasing the number of individuals protected through vaccination effectively reduces the probability of transmission within the population. Conversely, when the vaccination rate or vaccine effectiveness is lower, the infection curve rises more rapidly and reaches a higher peak, indicating faster outbreak development and a larger number of cases. Although the sensitivity analysis shows that vaccination parameters have a smaller effect on R_0 compared to some animal transmission parameters, increasing $v$and ϵ still contributes to reducing both R_0 and the overall number of infections. Therefore, improving vaccination coverage and vaccine effectiveness remains an important strategy for controlling monkeypox transmission, particularly when combined with other interventions such as case isolation and control of zoonotic transmission.

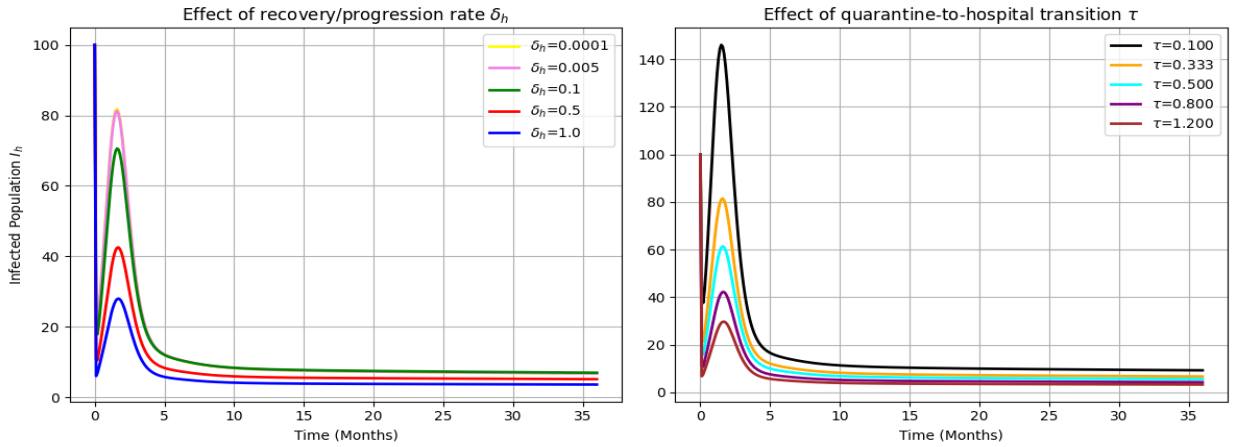

Figure 6. Population dynamics infected in the δ_h and τ scenarios.

Figure 6 shows that changes in the disease-induced mortality rate δ_h influence the infection dynamics by altering the duration of the infectious period. Higher values of $\delta_h$tend to reduce the peak number of infected individuals because infected individuals leave the infectious compartment more quickly due to disease-related deaths. However, this reduction does not represent an effective control strategy, as the decline in cases occurs due to increased mortality rather than reduced transmission. When $\delta_h$is lower, infected individuals remain infectious for a longer period, resulting in a higher peak and a longer outbreak duration. This increases the opportunity for transmission within the population. In contrast, variations in the treatment or isolation rate τshow a more desirable control pattern. Increasing τsignificantly reduces the peak number of infected individuals by accelerating the transition of infected individuals into treatment or isolation compartments. As a result, the duration of infectiousness is shortened, reducing the likelihood of further transmission in the community. Conversely, lower values of τlead to a rapid increase in infection levels because individuals remain infectious for a longer period. These findings suggest that improving early detection, treatment, and isolation measures is among the most effective strategies for reducing infection levels in the human population.

Implication to Health Resilience

The simulation results demonstrate that variations in key epidemiological parameters significantly influence the dynamics of infected humans $I_h(t)$. Transmission parameters $(\beta_h, \beta_r, \beta_1, \beta_2)$play a dominant role in determining the magnitude and timing of the epidemic peak. An increase in the human-to-human transmission rate $\beta_h$leads to a rapid rise in infection cases, while rodent-related transmission parameters β_r, β_1,and $\beta_2$highlight the important contribution of zoonotic reservoirs in sustaining disease spread. These findings indicate that both within-human and cross-species transmission pathways are critical in shaping outbreak dynamics, which is consistent with previous epidemiological and experimental studies (Americo et al., 2023; Dou et al., 2023). Intervention-related parameters show an inverse effect on disease transmission. Increasing the detection and isolation rate τ, as well as treatment and quarantine rates (θ_2, θ_3), reduces the infectious period and lowers the number of secondary infections. Higher vaccination rate v and vaccine effectiveness ϵcontribute to decreasing infection levels, although their impact on $R_0$is relatively smaller compared to transmission parameters. The rodent recovery rate γ_2 also plays a significant role in reducing R_0, emphasizing the importance of controlling infection within animal populations.

The findings are consistent with previous modeling studies that identify transmission rates and control measures as key determinants of monkeypox dynamics (Onifade et al., 2025; Qian et al., 2025; Pesantes-Grados et al., 2025). Many existing models focus primarily on human-to-human transmission. This study extends those approaches by incorporating bidirectional transmission between humans and rodents, allowing the identification of zoonotic feedback mechanisms that can amplify disease spread (Bolaji et al., 2024; Bunge et al., 2022). Similar patterns have also been reported in epidemiological investigations highlighting the role of zoonotic interactions and transmission networks (Yinka-Ogunleye et al., 2023; Thornhill et al., 2022). Several limitations

should be acknowledged. The model does not include age structure, which may influence contact patterns and susceptibility. Spatial heterogeneity is not considered, so geographic variation in transmission is not captured. Parameter uncertainty is not explicitly analyzed, since fixed parameter values are used. These assumptions may limit the ability of the model to fully represent real-world conditions.

The results provide important implications for public health policy in Indonesia. Reducing transmission rates, particularly those associated with rodent populations, is essential for controlling disease spread. Public health strategies may include improving environmental sanitation, strengthening rodent control programs, and increasing awareness of zoonotic transmission, which is consistent with studies highlighting the importance of public awareness in mpox prevention (El Sharif & Ahmead, 2025). Early detection and isolation strategies, represented by τ, remain critical for reducing transmission in the human population. Vaccination programs also contribute to outbreak mitigation when combined with other interventions. A coordinated approach across human health, environmental management, and community sectors is necessary to enhance resilience against zoonotic diseases, in line with global and national public health recommendations (WHO, 2024; Kemenkes, 2024).

CONCLUSION

This study developed a compartmental mathematical model describing monkeypox transmission dynamics between human and animal populations. The model incorporates key epidemiological processes, including natural birth and death, human-to-human and animal-to-human transmission, as well as intervention measures such as vaccination, isolation, and treatment. The human population is divided into the compartments S, V, E, I, Q, H,and R, while the animal population consists of S, E, I,and R. Analytical investigation of the model was carried out by determining the disease-free and endemic equilibrium points. The basic reproduction number $R_0$was derived using the next-generation matrix method to evaluate the potential for disease transmission. The analysis shows that when $R_0 < 1$, the disease-free equilibrium is locally stable, indicating that the infection cannot persist in the population. When $R_0 > 1$, the endemic equilibrium exists and the disease may persist.

Sensitivity analysis indicates that transmission-related parameters have a substantial influence on the value of R_0, particularly those associated with human-to-human transmission and zoonotic transmission from animal reservoirs. Intervention-related parameters, including vaccination and isolation processes, also contribute to reducing transmission, although their relative influence is smaller compared with the main transmission parameters. Numerical simulations further illustrate how variations in key parameters affect the number of infected individuals. Reductions in transmission parameters, especially β_h, β_1,and β_2, lead to a noticeable decrease in outbreak magnitude. Increases in detection, isolation, treatment, and vaccination rates $(\tau, \theta_2, \theta_3, v, \epsilon)$contribute to lowering the infection peak and slowing disease spread. Interventions targeting animal reservoirs, represented by γ_2, also play an important role in reducing sustained transmission.

The results emphasize the importance of integrating human health interventions with strategies targeting animal reservoirs in controlling monkeypox transmission. The model provides a theoretical framework for understanding the interaction between human and zoonotic transmission pathways and offers insights that may support public health decision-making. Future research may extend this work by incorporating optimal control theory to determine cost-effective intervention strategies, introducing spatial structure to capture geographic heterogeneity, and calibrating the model using real outbreak data to improve predictive accuracy and policy relevance.

AUTHOR CONTRIBUTIONS

V.L.: Conceptualization, methodology, investigation, project administration, writing – original draft, and writing – review and editing. S.S.: Data collection, data curation, formal analysis, and visualization. Y.H.P.: Data curation, formal analysis, and writing – review and editing.

CONFLICT OF INTEREST

The authors declare that they have no conflicts of interest regarding the publication of this paper.

REFERENCES

Agbata, B. C., Cenaj, E., Dervishi, R., Danjuma, Y. J., Shior, M.-A., Abah, E., Onuche, J. S., & Emadifar, H. (2025). Fractional-order mathematical model for monkeypox transmission dynamics using the Atangana-Baleanu Caputo operator. *BMC Infectious Diseases, 25*(1), 1000. https://doi.org/10.1186/s12879-025-11383-7

Albericio, G., Rodríguez-Martín, D., Avilés, P., Cuevas, C., Guillén-Navarro, M. J., Noriega, M. A., Flores, S., Sánchez-Cordón, P. J., Astorgano, D., Pérez, P., Esteban, M., & García-Arriaza, J. (2025). Functional characteristics of plitidepsin as an antiviral treatment against monkeypox virus infection. *Antiviral Research, 241*, 106238. https://doi.org/10.1016/j.antiviral.2025.106238

Allehiany, F. M., DarAssi, M. H., Ahmad, I., Khan, M. A., & Tag-eldin, E. M. (2023). Mathematical modeling and backward bifurcation in monkeypox disease under real observed data. *Results in Physics, 50*, 106557. https://doi.org/10.1016/j.rinp.2023.106557

Americo, J. L., Earl, P. L., & Moss, B. (2023). Virulence differences of mpox (monkeypox) virus clades I, IIa, and IIb.1 in a small animal model. *Proceedings of the National Academy of Sciences*, 120, e2220415120. https://doi.org/10.1073/pnas.2220415120

Bolaji, L. K., Sagir, A. M., & Balogun, F. (2024). Mathematical transmission dynamics and intervention strategies for monkeypox: A model-based approach including human–rodent interactions. *UMYU Scientifica, 3*(4), 288–299. https://doi.org/10.56919/usci.2434.023

Brauer, F., Castillo-Chavez, C., & Feng, Z. (2019). *Mathematical models in epidemiology*. Springer. https://doi.org/10.1007/978-1-4939-9828-9

BPS-Statistics Indonesia. (2024). Indonesia's human development index (HDI) in 2024 reached 75.02.

Bunge, E. M., Hoet, B., Chen, L., Lienert, F., Weidenthaler, H., Baer, L. R., & Steffen R. (2022). The changing epidemiology of human monkeypox—A potential threat? A systematic review. *PLoS Neglected Tropical Diseases, 16*(2), e0010141. https://doi.org/10.1371/journal.pntd.0010141

Chen, Z., Zhang, L., Li, L., Shao, M., Zhao, Z., Shang, C., Liu, Z., Liu, J., Liu, Y., Li, X., & Guo, Z. (2026). Pathogenicity and transmissibility of Mpox virus in African dormice. *Microbiology Spectrum, 14*(2), e0192625. https://doi.org/10.1128/spectrum.01926-25

Cordeiro, R., Batista, F. da C., Pelerito, A., Carvalho, I. L. de, Lopo, S., Neves, R., Rocha, R., Palminha, P., Borrego, M. J., Núncio, M. S., & Gomes, J. P. (2025). Undetected circulation of monkeypox virus in Portugal: Evidence for a 50-day gap before first detection. *Global Epidemiology*. https://doi.org/10.1016/j.gloepi.2025.100238

De Baetselier, I., Van Dijck, C., Kenyon, C., Coppens, J., Michiels, J., De Block, T., Smet, H., Coppens, S., Vanroye, F., Bugert, J. J., Girl, P., Zange, S., Liesenborghs, L., Brosius, I., Griensven, J., Selhorst, P., Florence, E., Bossche, D. V., Ariën, K. K., Rezende, A. M., Vercauteren, K., & Esbroeck, M. (2022). Retrospective detection of asymptomatic monkeypox virus infections among male sexual health clinic attendees in Belgium. *Nature Medicine*, 28, 2288–2292. https://doi.org/10.1038/s41591-022-02004-w

Demir, M. (2025). Modeling monkeypox: Spread of outbreak with social distancing, quarantine and vaccination. *Bitlis Eren Üniversitesi Fen Bilimleri Dergisi, 14*(1), 361–384. https://doi.org/10.17798/bitlisfen.1589786

Deputy, N. P., Deckert, J., Chard, A. N., Sandberg, N., Moulia, D. L., Barkley, E., Dalton, A. F., Sweet, C., Cohn, A. C., Little, D. R., Cohen, A. L., Sandmann, D., Payne, D. C., Gerhart, J. L., & Feldstein, L. R.. (2023). Vaccine effectiveness of JYNNEOS against mpox disease in the United States. *New England Journal of Medicine*, 388, 2434–2443. https://doi.org/10.1056/NEJMoa2215201

Direktorat Jenderal Pencegahan dan Pengendalian Penyakit. (2023). *Pedoman pencegahan dan pengendalian mpox (monkeypox)*. Kementerian Kesehatan RI.

Direktorat Jenderal Pencegahan dan Pengendalian Penyakit. (2024). *Technical report mpox di Indonesia tahun 2023*. Kementerian Kesehatan RI.

Dou, X., Li, F., Ren, Z., Zhang, D., Li, J., Li, D., Sun, Y., Jin, H., Li, R., Li, W., Zhang, X., Yang, Y., Jia, L., Yu, H.,

Li, W., &Pan, Y. (2023). Clinical, epidemiological, and virological features of Mpox in Beijing, China – May 31–June 21, 2023. *Emerging Microbes & Infections*, 12, 2254407. https://doi.org/10.1080/22221751.2023.2254407

El Moujaddid, S., Harroudi, S., & Allali, K. (2025). Monkeypox disease with saturated incidence rates: Mathematical analysis. *Gulf Journal of Mathematics, 20*(2). https://doi.org/10.56947/gjom.v20i2.3248

El Sharif, N., & Ahmead, M. (2025). Assessment of knowledge and awareness of monkeypox viral infection in Palestine: A community-based study. *Frontiers in Cellular and Infection Microbiology, 15*, 1584848. https://doi.org/10.3389/fcimb.2025.1584848

Ernest-Okonofua, E. O., Zubairu, Z. A., Oduoye, M. O., Tariq, M., Muhammad, S., Siddiqua, Z., Vuyyuru, M., Wafula, B., Akhtar, R., Fasasi, A., Ubechu, S. C., & Olayinka, B. S. (2025). Harnessing artificial intelligence and innovative vaccines for mpox diagnosis and control: A comprehensive narrative review. *Journal of Primary Care & Community Health, 16*, 21501319251357701. https://doi.org/10.1177/21501319251357701

Halder, S., Panda, S., Samadder, A., & Chattopadhyay, J. (2025). Enhancing Disease Control in Resource-Limited Settings Through Bidirectional Behavioral Responses. *Bulletin of Mathematical Biology, 87*(10), 149. https://doi.org/10.1007/s11538-025-01514-1

Herate, C., Ferrier-Rembert, A., Relouzat, F., Gallouët, A-S., Pascal, Q., Delache, B., Langlois, S., Timera, H., Jarjaval, F., Bossevot, L., Ludot, C., Brua, C., Lechemia, M., Ferraris, O., Silvestre, N., Le Grand, R., & Tournier, J-N. (2025). Efficacy of modified-vaccinia Ankara vaccine as pre- and post-exposure prophylaxis against monkeypox sexual transmission in non-human primate model. *Nature Communications, 16*(1), 7306. https://doi.org/10.1038/s41467-025-62681-2

Azeez, T. A., Adetunji, T. A., & Adio, M. (2022). Thyrotoxicosis in Africa: A systematic review and meta-analysis of the clinical presentation. *The Egyptian Journal of Internal Medicine, 34*, 57. https://doi.org/10.1186/s43162-022-00145-5

Jin, S., Guan, T., Endo, A., Gan, G., Janhavi, A., Hu, G., Ejima, K., Lim, J. T., & Dickens, B. L. (2025). Effectiveness of different border control strategies for reducing mpox importation risk: a modelling study. *The Lancet Regional Health – Southeast Asia, 35*, 100565. https://doi.org/10.1016/j.lansea.2025.100565

Joshi, S., Kumar, R., Dwivedi, A., Kumar, A., Rai, P. K., & Amrita. (2025). An Adaptive Generative 3D VNet Model for Enhanced Monkeypox Lesion Classification Using Deep Learning and Augmented Image Fusion. *Journal of Imaging Informatics in Medicine*. https://doi.org/10.1007/s10278-025-01594-4

Kannan, S., Shaik Syed Ali, P., & Sheeza, A. (2022). Monkeypox: Epidemiology, transmission, clinical features, and molecular properties. *European Review for Medical and Pharmacological Sciences*, 26, 5983–5990.

Keeling, M. J., & Rohani, P. (2019). *Modeling infectious diseases in humans and animals*. Princeton University Press.

Kementerian Kesehatan Republik Indonesia (Kemenkes). (2024). *Laporan penilaian risiko cepat mpox di Indonesia tahun 2024*.

Li, T., Guo, X., Wang, X., & Chen, T. (2025). Temporal and age-structured analysis of Mpox spread in the 2022 Global outbreak: data-assimilation insights for epidemic control. *Infectious Diseases of Poverty, 14*(1), 100. https://doi.org/10.1186/s40249-025-01369-7

Merad, Y., Godinot, M., Alfaiate, D., Becker, A., Ader, F., Cotte, L., & Conrad, A. (2025). Determinants of mpox vaccination uptake among MSM during the 2022 outbreak: a single-centre retrospective study at Lyon University Hospital, France. *BMC Public Health, 25*(1), 3496. https://doi.org/10.1186/s12889-025-24728-3

Nilasari, H., Miranda, E., Marissa, M., Ruspitawati, A., Handayani, D. O. T. L., Salama, N., Setiawan, B., Supriadi, Aisyah, T. V., Inggriwati, Haq, A. S., Zuhroh, S., Safitri, E. Y., Pramono, R. A., Wisnuwardani, I., Nelwan, E. J., Sinto, R., Susilo, A., Saharman, Y. R., Ratnoglik, S. L., Pitawati, N. L. P., Fauzan, M., Hasanah, S. S. A., Sharasti, M., & Yunihastuti, E. (2025). Epidemiology and Clinical Features of Mpox in Jakarta, Indonesia, August 2022–December 2023. *Vaccines, 13*(3), 210. https://doi.org/10.3390/vaccines13030210

Nivetha, S., Das, P., & Ghosh, M. (2025). Threshold dynamics and epidemic-informed machine learning for forecasting of mpox: A U.S. case study. *Chaos, 35*(11), 113118.

https://doi.org/10.1063/5.0299032
Omame, A., Iyaniwura, S. A., Han, Q., Ebenezer, A., Bragazzi, N. L., Wang, X., Woldegerima, W. A., & Kong, J. D. (2025). Dynamics of Mpox in an HIV endemic community: A mathematical modelling approach. *Mathematical Biosciences and Engineering, 22*(2), 225–259. https://doi.org/10.3934/mbe.2025010
Onifade, A. A., Akindele, O. A., Ahmad, I., Khan, M. A., Isa, N. M., & Alzahrani, E. (2025). Modeling monkeypox transmission with a compartmental framework to evaluate testing, isolation and public awareness strategies. *Scientific Reports, 15*, 27236. https://doi.org/10.1038/s41598-025-10852-y
Pesantes-Grados, P., Escalante-Ccoyllo, N., Marín-Machuca, O., Zambrano-Cabanillas, A. W., Ango-Aguilar, H., Marín-Sánchez, O., & Chacón, R. D. (2025). A Compartmental Mathematical Model to Assess the Impact of Vaccination, Isolation, and Key Epidemiological Parameters on Mpox Control. *Medical Sciences, 13*(4), 226. https://doi.org/10.3390/medsci13040226
Prévost, J., Tailor, N., Soule, G., Medina, S. J., Tierney, K., Azaransky, K., & Safronetz, D. (2026). Pathogenicity and antiviral treatment of clade Ib Monkeypox virus infection in mice. *Antiviral Research, 248*, 106377. https://doi.org/10.1016/j.antiviral.2026.106377
Qian, M., Li, D., Hao, Z., Hu, S., & Li, W. (2025). An epidemiological model of monkeypox: model prediction and control application. *BMC Infectious Diseases, 25*(1), 1000. https://doi.org/10.1186/s12879-025-10873-y
Rossotti, R., Calzavara, D., Cernuschi, M., D'Amico, F., De Bona, A., Repossi, R., Moschese, D., Bossolasco, S., Tavelli, A., Muccini, C., Mulé, G., & Monforte, A. d. (2023). Detection of Asymptomatic Mpox Carriers among High-Ri Men Who Have Sex with Men: A Prospective Analysis. *Pathogens*, 12, 798. https://doi.org/10.3390/pathogens12060798
Su, W., Zhao, T., Ren, X.,Li, S., Huang, Q., Liu, J., Zhang, X., Ge, Z., & Wei, J. (2026). Protective efficacy of a genetically modified attenuated vaccinia virus Tiantan strain against monkeypox virus challenge in a small animal model. *Journal of Virology, 100*(2), e0184325. https://doi.org/10.1128/jvi.01843-25
Tenrisau, D., Purnama, T. B., Maulana, M. A. W., Ahsani, R. F., Mulya, H. K., Maladan, Y., Azizah, L., Caloh, G. B. A., & Kasim, F. (2025). Molecular epidemiology of mpox in Indonesi from 2023 to 2024. *Epidemiology and Infection, 153*, e79. https://doi.org/10.1017/S0950268825100253
Tian, L., Qin, H., Li, S., Zhang, M., Zhuang, L., Hong, B., Liu, K., Li, M., Li, S., Wang, Y., Song, L., Liu, Y., Wang, Y., Liu, H., Tong, Y., & Fan, H. (2026). Lactoferrin as antiviral against orthopoxvirus. *Emerging Microbes & Infections, 15*(1), 2631205. https://doi.org/10.1080/22221751.2026.2631205
Thornhill, J. P., Barkati, S., Walmsley, S., Rockstroh, J., Antinori, A., Harrison, L. B., Palich, R., Nori, A., Reeves, I., Habibi, M. S., et al. (2022). Monkeypox virus infection in humans across 16 countries. *New England Journal of Medicine*, 387, 679–691. https://doi.org/10.1056/NEJMoa2207323
Wang, X., & Lun, W. (2023). Skin manifestations of human monkeypox. *Journal of Clinical Medicine*, 12, 914. https://doi.org/10.3390/jcm12030914
World Health Organization (WHO). (2024). Mpox (monkeypox) outbreak.
Wu, S., Deng, J., Du, M., Liu, M., & Liu, J. (2025). Mpox vaccination hesitancy and its associated factors among the general population in China: A national observational study. *Human Vaccines & Immunotherapeutics, 21*(1), 2523636. https://doi.org/10.1080/21645515.2025.2523636
Xu, C., Zhang, J., Xu, H., Gao, Y., Liu, S., Xu, L., Hu, F., Xu, G., Wang, Y., & Cai, Y. (2025). Using protection motivation theory to explain monkeypox vaccination intention among men who have sex with men in China. *BMC Medicine, 23*(1), 652. https://doi.org/10.1186/s12916-025-04473-5
Yinka-Ogunleye, A., Dalhat, M., Akinpelu, A., Aruna, O., Garba, F., Ahmad, A., Adeleye, A., Botson, I., Oluwafemi, B., Ogunbode, O., Amao, L., Ekripo, U., Aliyu, G. G., Adetifa, I., Ihekweazu, C., & Abubakar, I. (2023). Mpox risk and mortality associated with HIV infection: a national case–control study in Nigeria. *BMJ Global Health*, 8, e013126. https://doi.org/10.1136/bmjgh-2023-013126
Zhang, X.-S., Niyomsri, S., Mandal, S., Mohammed, H., Mindlin, M., Dugbazah, B., Adjei, S., Owoseni, B., Charlett, A., I'Anson, J., Sugars, E., Kliner, M., Mannes, T., Jewitt, E., Gilbert, L., Moazam, S., Dewsnap, C., Phillips, D., Amirthalingam, G., Ramsay, M. E., Vickerman, P., & Walker, J. G. (2025). Cost-effectiveness of vaccination strategies to control future mpox outbreaks in England: a

modelling study. *The Lancet Regional Health – Europe, 55*, 101364. https://doi.org/10.1016/j.lanepe.2025.101364